Geophysical Research Letters

RESEARCH LETTER
10.1029/2021GL096965

# Ultra-Oligotrophic Waters Expansion in the North Atlantic Subtropical Gyre Revealed by 21 Years of Satellite Observations

F. E. Leonelli[1,2], M. Bellacicco[1], J. Pitarch[1], E. Organelli[1], B. Buongiorno Nardelli[3], V. de Toma[4,5], C. Cammarota[2], S. Marullo[1,5], and R. Santoleri[1]

[1]National Research Council of Italy (CNR), Institute of Marine Sciences (ISMAR), Rome, Italy, [2]Department of Mathematics Guido Castelnuovo, University of Rome La Sapienza, Rome, Italy, [3]National Research Council of Italy (CNR), Institute of Marine Sciences (ISMAR), Naples, Italy, [4]Department of Physics & INFN, University of Rome "Tor Vergata", Rome, Italy, [5]Italian National Agency for New Technologies, Energy, and Sustainable Economic Development (ENEA), Frascati, Italy

**Key Points:**

- The lowest chlorophyll-*a* waters in the North Atlantic Subtropical Gyre (NASTG) are spatially expanding and increasing in frequency, as seen by 21 years of satellite data
- NASTG core shows a shift to a dominant quasi-permanent ultra-oligotrophic condition
- Ocean warming's role in sharpening oligotrophy is more complex than local stratification increase only

**Supporting Information:**

Supporting Information may be found in the online version of this article.

**Correspondence to:**

M. Bellacicco,
marco.bellacicco@artov.ismar.cnr.it

**Citation:**

Leonelli, F. E., Bellacicco, M., Pitarch, J., Organelli, E., Buongiorno Nardelli, B., de Toma, V., et al. (2022). Ultra-oligotrophic waters expansion in the North Atlantic Subtropical Gyre revealed by 21 years of satellite observations. *Geophysical Research Letters*, *49*, e2021GL096965. https://doi.org/10.1029/2021GL096965

Received 11 NOV 2021
Accepted 24 SEP 2022

**Author Contributions:**

**Conceptualization:** F. E. Leonelli, M. Bellacicco, S. Marullo
**Data curation:** F. E. Leonelli, V. de Toma, S. Marullo
**Formal analysis:** F. E. Leonelli, M. Bellacicco, J. Pitarch, E. Organelli, S. Marullo
**Funding acquisition:** R. Santoleri
**Investigation:** F. E. Leonelli, M. Bellacicco, J. Pitarch, E. Organelli, B. Buongiorno Nardelli, S. Marullo
**Methodology:** F. E. Leonelli, M. Bellacicco, J. Pitarch
**Supervision:** M. Bellacicco, S. Marullo
**Validation:** F. E. Leonelli



**Abstract** The North Atlantic Subtropical Gyre (NASTG) has experienced the fastest expansion of oligotrophic waters worldwide in response to ocean warming. We study the trophic regime changes in the NASTG by using 21 years (1998–2018) of satellite chlorophyll-*a* (CHL) data, complemented with other variables such as Sea Surface Temperature, optical backscatter coefficients ($b_{bp}$), Secchi disk ($z_{SD}$), and Mixed Layer Depth. To this aim, we describe the spatial/temporal variability of waters with the lowest CHL concentrations (CHL $\leq$ 0.04 mg m$^{-3}$) with an inter-annual variability analysis of key environmental variables. Main results demonstrate that these ultra-oligotrophic waters are spatially expanding and increasing in frequency, shifting the NASTG to a dominant quasi-permanent ultra-oligotrophic condition, thus confirming the ongoing ocean desertification.

**Plain Language Summary** Oceanic subtropical gyres have a fundamental role in the global carbon budget due to their immense ecosystem size even if they are characterized by oligotrophic waters. In the last decades, the North Atlantic Subtropical Gyre (NASTG) has experienced the fastest expansion of oligotrophic waters worldwide with an enlargement in response to the ongoing ocean warming. Here, we study the trophic regime changes in the NASTG by using 21 years (1998–2018) of satellite phytoplankton chlorophyll-*a* (CHL) data, complemented with other environmental variables such as Sea Surface Temperature, suspended particle concentration, water transparency, and Mixed Layer Depth. To this main goal, we describe the spatial and temporal variability of waters characterized by CHL $\leq$ 0.04 mg m$^{-3}$ together with an inter-annual variability analysis of the key oceanic variables introduced. The main findings demonstrate that these ultra-oligotrophic waters are spatially expanding and increasing in frequency, shifting the NASTG to a dominant quasi-permanent ultra-oligotrophic condition, confirming the ongoing impactful ocean desertification.

## 1. Introduction

The key contribution of the oceanic subtropical gyres in defining the global carbon budget is well recognized (Dave et al., 2015). Globally, the subtropical gyres occupy approximately 40% of the surface of the Earth and are characterized by oligotrophic conditions, that is having weak supply of new nutrients, low phytoplankton biomass and primary production at the surface (Polovina et al., 2008). Despite this trophic condition and their consequent relatively weak and inefficient export of carbon from the euphotic zone (Henson et al., 2012), they do anyway significantly contribute to the global export production because of their immense ecosystem size (Dave et al., 2015; Polovina et al., 2008).

The North Atlantic Subtropical Gyre (NASTG) is bounded on the northern side by the more productive waters of the subpolar gyre, while, conversely, the southeastern and southwestern borders reflect the West African coastal upwelling zone and the Amazon outflow region, respectively. Oligotrophic conditions, historically set with surface chlorophyll-*a* concentration (CHL; mg m$^{-3}$) values $\leq$0.1 mg/m$^{-3}$ (sometimes delimited by CHL $\leq$ 0.07 mg m$^{-3}$), are mostly in the central and western portions of the gyre. A lobe of the oligotrophic waters extends also south toward the tropics. Seasonally, the oligotrophic waters expand in summer, largely coinciding with the area of the NASTG, while they contract considerably during the winter season (Figure 1). Such seasonal change is strongly identified by the northward/southward shift of the boundary between the NASTG and the subpolar region, which

Geophysical Research Letters 10.1029/2021GL096965

**Writing – original draft:** F. E. Leonelli, M. Bellacicco, J. Pitarch, E. Organelli, V. de Toma, S. Marullo
**Writing – review & editing:** F. E. Leonelli, M. Bellacicco, J. Pitarch, E. Organelli, B. Buongiorno Nardelli, V. de Toma, C. Cammarota, S. Marullo

is to be considered as defined by the separatrix of the geostrophic stream function (Dave et al., 2015; see their Figure 1).

In the last decades, several studies based on satellite observations have suggested that oligotrophic waters are experiencing a geographical increase in response to ocean warming (e.g., Irwin & Oliver, 2009). In this regard, the concurrent increase of Sea Surface Temperature (SST) and decrease of phytoplankton biomass has been widely documented (Gregg & Conkright, 2002; Gregg et al., 2005; Martinez et al., 2009). Polovina et al. (2008) reported that, from 1998 until 2006, the oligotrophic waters (defined as those verifying the condition CHL $\leq 0.07$ mg $m^{-3}$) within the subtropical gyres of the major oceans (e.g., Atlantic and Pacific) had been expanding at average yearly rates between 0.8% and 4.3%/yr, mainly during the winter season and in response to the increase of SST. In particular, the fastest expansion of oligotrophic waters worldwide was observed within the area of the NASTG, which experienced an enlargement of around 56% between 1998 and 2006, causing substantial impacts on the entire North Atlantic Ocean ecosystem (i.e., decrease of primary production; Behrenfeld et al., 2006).

Long-term changes in ocean biology of the NASTG have been previously studied by means of satellite CHL observations with limited time coverage (e.g., 1997–2008 in Behrenfeld et al., 2006; 1998–2006 in Polovina et al., 2008; 1998–2010 in Siegel et al., 2013). However, it has been well demonstrated that satellite CHL alone cannot always give a reliable estimation of phytoplankton concentration in the subtropical gyres, being strongly influenced by physiological processes (i.e., photoacclimation) (Bellacicco et al., 2020; Siegel et al., 2013). Photoacclimation is the phytoplankton response to fluctuations in light, nutrients, and temperature with physiological strategies that enhance the efficiency of light capturing and photosynthetic capacity, growth, and persistence by the regulation of the pigment amounts (e.g., CHL) and other components of the photosynthetic machinery (e.g., electron transport chain). It can be detected from space by the use of the phytoplankton CHL to carbon biomass (CHL:$C_{phyto}$) ratio (Behrenfeld et al., 2015; Halsey & Jones, 2015). In addition to this, a robust detection of long-term changes would require climatologies to be computed on a time series covering a period of at least 30 years (WMO, 2017), allowing with such length of observations to have a robust identification of typical values to refer to. It derives that most previous studies based on the use of satellite CHL time-series with a reduced length had critical caveats for reliable climate change interpretations (Dutkiewicz et al., 2019).

This work revisits the ocean biology and trophic regime changes in the NASTG by using 21 years (1998–2018) of satellite time series of CHL, which is analyzed together with other variables such as SST, particulate optical backscatter coefficient ($b_{bp}$, $m^{-1}$), Secchi disk depth ($z_{SD}$, m), and Mixed Layer Depth (MLD; m). $b_{bp}$ is an inherent optical property related to the particle concentration in seawater and to the size distribution, refractive index, shape, and structure (Stramski et al., 2004). Most of $b_{bp}$ in open clear waters is due to particles with equivalent diameters between 1 and 10 μm (Organelli et al., 2018), thus including the contribution of pico- and nano-phytoplankton and non-algal particles (Organelli et al., 2020). Since $b_{bp}$ is commonly used as a proxy of $C_{phyto}$ (Behrenfeld et al., 2005), it enables the characterization of phytoplankton physiological strategies, coupled with CHL, giving thus new insight on phytoplankton dynamics both in space and time. To complement the optical view of the NASTG, we also include $z_{SD}$, which partly correlates to $b_{bp}$, but is also influenced by light absorption by suspended particles and dissolved substances, thus being a measure of water transparency and directly related to diffuse light attenuation (Lee et al., 2015). Finally, MLD provides information on vertical mixing and, if deep enough to reach the nutricline, on potential nutrient supply from the deeper layers also.

We describe the temporal variability of waters with low CHL concentrations using satellite observations, exploring different criteria for their definition. Then, we describe the spatial variability of the waters characterized by the least CHL concentrations for the entire period and, lastly, we analyze the inter-annual variability of key environmental variables in the area thus found to better characterize long-term ocean biology changes in the NASTG.

## 2. Data and Methods

### 2.1. OC Data Sets

We use the extensive time series of Ocean Color (OC) data (1998–2018) from the European Space Agency (ESA) OC Climate Change Initiative (CCI) project (Sathyendranath et al., 2019) v4.2 Level 3 (gridded). The ESA OC-CCI project aims at creating a long-term, consistent, uncertainty-characterized time series of OC products, to be used in climate-change studies. OC-CCI products result from the merging of SeaWiFS, MERIS, MODIS, and VIIRS data, and in version 4.2 here used the inter-sensor biases are removed respect to previous versions

10.1029/2021GL096965

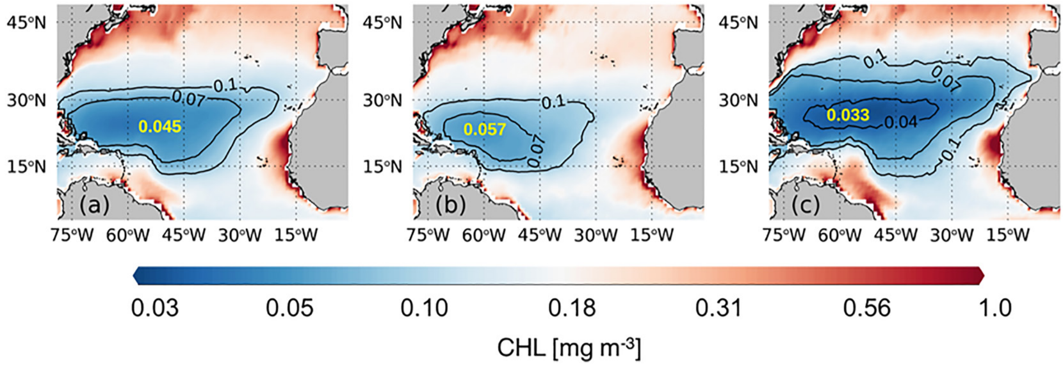


**Figure 1.** (a) Annual, (b) Winter (December, January, and February), and (c) Summer (June, July, and August) mean of chlorophyll-*a* (CHL) for the period 1998–2018. Black contour lines indicate CHL isolines for 0.04, 0.07, and 0.1 mg $m^{-3}$ thresholds. CHL minima is reported in yellow.

including the latest NASA reprocessing R2018.0 that mostly accounts for the aging of MODIS (https://docs.pml.space/share/s/dPL4zFuaT_eFa-mTLU9nQA).

We downloaded daily CHL data at 4 km resolution from the ESA OC-CCI portal, and added the corresponding bias for each value. Extensive explanations about the bias application can be found in Sathyendranath et al. (2019). We downloaded daily Remote Sensing Reflectance ($R_{rs}$; in $sr^{-1}$) time-series at 4 km resolution from the ESA OC-CCI portal over the area of study adding the corresponding bias. Daily $R_{rs}$ were then used to compute monthly $b_{bp}$ at 443 nm after the application of the QAA algorithm with Raman correction included, following the recommendations in Pitarch et al. (2020), which increased the accuracy of retrievals. $z_{SD}$ monthly data for the period 1998–2018 were downloaded from PANGAEA (Pitarch et al., 2019, 2021), where the data were estimated by applying Lee et al. (2015) algorithm on OC-CCI v4.2 $R_{rs}$ data.

All OC variables (CHL, $b_{bp}$, and $z_{SD}$) are derived from the same ESA OC CCI daily $R_{rs}$, but result from different algorithms, which may affect space-time data coverage of individual variables (see Figure S1 and Table S1 in Supporting Information S1).

### 2.2. SST Data Set

We use the ESA-CCI SST data set v2.0, which provides global daily satellite-based SST data covering the period from September 1981 to present, distributed in the Climate Data Record (CDR). The data set is designed to provide a long-term, stable, low-bias CDR derived from different infrared sensors, that is, the AVHRR, (A)ATSR, and SLSTR series of sensors (Merchant et al., 2014, 2019). We download the Level 4 product v2.0, which consists of spatially complete (optimally interpolated) maps of global daily average SST at 20 cm nominal depth at 0.05° × 0.05° regular grid (Donlon et al., 2012).

### 2.3. MLD Data Set

MLD data were extracted from the ARMOR3D Level 3 reprocessed data set, which is an observation-based 4D reconstruction of the global ocean state obtained from the combination of in situ and satellite data (Guinehut et al., 2012), and provides weekly fields of different variables at a nominal 0.25° latitude-longitude resolution, over 50 vertical levels from the surface down to 5,500 m depth (see Supporting Information S1). It is disseminated by the Copernicus Marine Service (CMEMS) (see CMEMS-Product User Manual).

Here, all variables have been remapped to a common 1° × 1° spatial grid sufficient to resolve the broader oceanographic scales of variability for the common period 1998–2018. The Multivariate Singular Spectral Analysis method is used to fill the gaps of the L3 data sets used for the study: Chl, $b_{bp}$, $z_{SD}$, and MLD. All monthly data sets interpolated present a low fraction of average gaps (Figures S1, S2 and Table S1 in Supporting Information S1). For mathematical and more details see Supporting Information S1 and Ghil et al. (2002), Kondrashov and Ghil (2006), and Kondrashov et al. (2010).

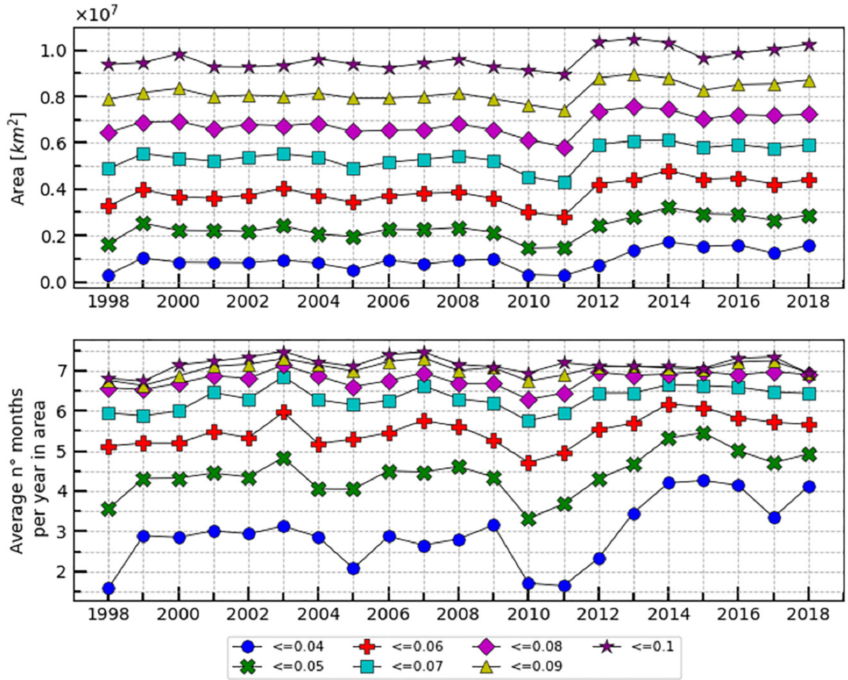


**Figure 2.** Annual average area characterized by values chlorophyll-*a* ≤ 0.04–0.1 mg m$^{-3}$ (upper panel) and average annual number of months when such oligotrophic conditions occur (lower panel) for the period 1998–2018 in the North Atlantic Subtropical Gyre.

## 3. Results and Discussion

The changes of the temporal evolution in CHL data for the entire period 1998–2018 are inspected while defining CHL thresholds in the range of values between 0.04 and 0.1 mg m$^{-3}$. Our aim is to understand which threshold better defines the waters which experience the most impactful changes in the last decades. The average annual area characterized by CHL values less or equal than the different thresholds together with the average number of months through the year when such oligotrophic conditions occur are shown in Figure 2. If all threshold choices exhibit a general increase tendency in the area coverage (upper panel of Figure 2), it is worth noting how the most ultra-oligotrophic waters (i.e., CHL ≤ 0.04 mg m$^{-3}$) are the ones which experience the highest percentage difference when comparing the average value of the last and the first 4 years of observations. Indeed, if the area with CHL values ≤0.1 mg m$^{-3}$ experiences a growth of 4.9% and observations of CHL ≤ 0.07 mg m$^{-3}$ experience an increase of 11.5%, the ultra-oligotrophic waters being CHL ≤ 0.04 mg m$^{-3}$ show an increase of 96.3%. This discrepancy is also confirmed in terms of rates of change per year having 21.6% for the 0.04 mg m$^{-3}$ limit compared to 1.4% and 0.5% for the 0.07 and 0.1 mg m$^{-3}$ limits, respectively. The fact that the ultra-oligotrophic waters are the most sensitive to an increase in the 1998–2018 period is even more evident when observing the average annual occurrences (lower panel of Figure 2). Indeed, if observations with values less or equal to 0.04 mg m$^{-3}$ would arise on average twice a year in the initial years, at the end of the period we see approximately a doubling of average occurrences per year. In other words, when considering the first and last 4 years, the percentage increase of average ultra-oligotrophic occurrences is 53.8% compared to 7.6% for 0.07 mg m$^{-3}$, and to 2.6% for 0.1 mg m$^{-3}$ (as before, these results are shown to be robust for rates of changes per year, Table S2 in Supporting Information S1 for details). This outcome is not affected by data availability before gap-filling is performed, indeed the ≤0.04 mg m$^{-3}$ waters show no direct correlation with the monthly CHL valid observations (Figure S3 in Supporting Information S1). Also, by excluding the 1998 values, which are very low if compared with subsequent years, the difference between the thresholds' percentage changes of area and annual occurrences remains sharp (Table S2 in Supporting Information S1). This leads us to choose the 0.04 mg m$^{-3}$ limit for deepening our understanding of the ultra-oligotrophic regime evolution, differing from Polovina et al. (2008) and Dave et al. (2015) where a similar analysis was conducted using the threshold of CHL of 0.07 mg m$^{-3}$. In this respect,

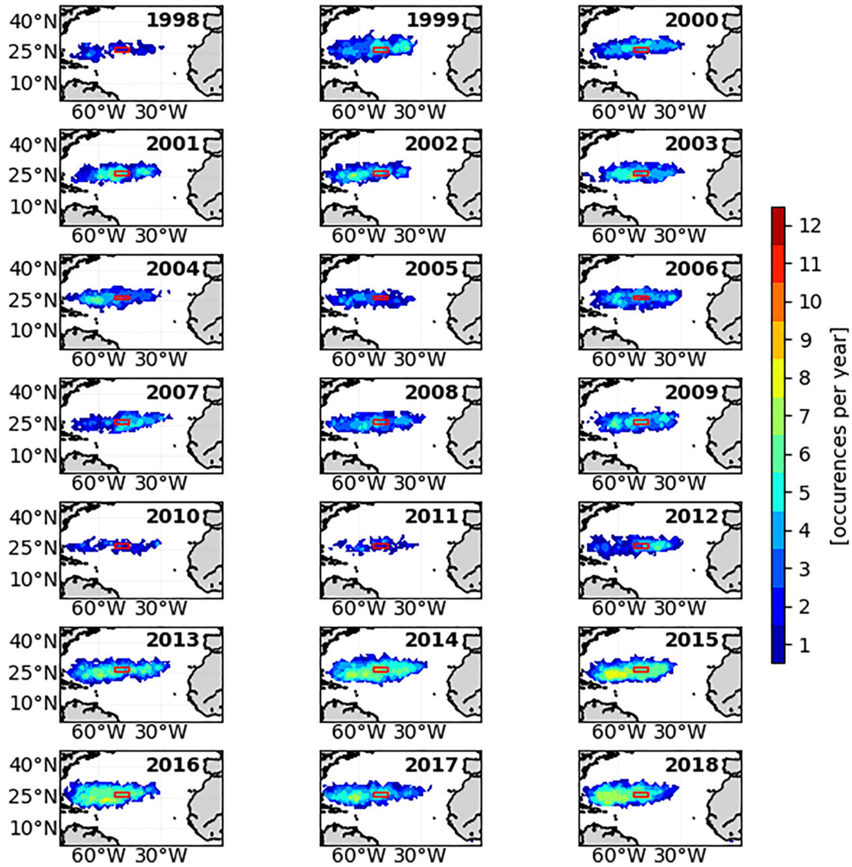


**Figure 3.** Area characterized by chlorophyll-$a \leq 0.04$ mg m$^{-3}$ for the period 1998–2018 in the North Atlantic Subtropical Gyre. The average number of months per year when this condition is verified is depicted as pixel color. The largest box having non-null occurrences during all years is in red.

for the 0.07 mg m$^{-3}$ limit, occurrences are seen to be fairly stable around 6 months per year and exhibiting only a slight increase in the period under study.

Spatially, the observations of waters characterized by the 0.04 mg m$^{-3}$ limit from 1998 until 2018 are confined to the NASTG from 1998 until 2018 (Figure 3), concentrated in the core of the gyre as expected for this area (Gregg et al., 2005). From 1999 to 2009, the occurrence of such conditions became more frequent with an average of four to five monthly observations per year, reaching in some areas peaks of 7–8 months per year. In other words, if the ultra-oligotrophic regime initially appears as an infrequent condition, with a restricted spatial expansion and low annual average pixel-wise occurrences, by the end of the time series it occurs for half of the year on average and covers a wider area in the core of the NASTG.

Both figures also highlight the non-linearity of the changes that have affected the NASTG throughout the period of study. In 2010 and 2011, there was an abrupt increase of CHL and a subsequent decrease of ultra-oligotrophic waters within the NASTG. Indeed, in these years, CHL takes the highest values of the entire time series. Then, from 2013 onwards, the ultra-oligotrophic waters returned to prevail in the core of the NASTG with a strong and faster geographical expansion combined with a rise of annual pixel-wise frequency, equal or greater than 6 months in the last years of the series. Therefore, the variations in shape and size of the area delimiting the clearest waters, are accounting for a shift to a dominant quasi-permanent ultra-oligotrophic condition of the NASTG's core. By using the other thresholds, such as the 0.07 or 0.1 mg m$^{-3}$ (Gregg et al., 2005; McClain et al., 2004) those spatial and temporal expansions could not be observed, not allowing for a real comprehension of the actual ocean desertification of the NASTG.

With the objective of achieving a more effective picture of the ocean biology and regime changes in the area identified by values of CHL $\leq 0.04$ mg m$^{-3}$, namely responding to the ultra-oligotrophic condition, here we describe

10.1029/2021GL096965

the inter-annual variability of additional essential oceanic variables over the period of analysis (Figure 4; Figure S4 in Supporting Information S1).

Annual averages of CHL (Figure 4; continuous lines) steadily range around 3.6–3.7·$10^{-2}$ mg $m^{-3}$ until 2010, reaching the maximum values (∼3.8 mg $m^{-3}$) during the 2010–2012 years, in correspondence with SST lowest values (∼22.5°C), and then experiencing a sharp decrease until 2018, again concurrent to the rise of SST which reaches its maximum value on average (∼23.8°C). Indeed, SST and CHL for the ultra-oligotrophic waters are highly anti-correlated (−0.65), while for the other limits this relation is not encountered as sharp (−0.33; Figure S4 in Supporting Information S1). This is consistent with previous works based on satellite observations (Behrenfeld et al., 2006) and in-situ measurements in which a decrease of CHL and chlorophyll-*b*, as well as primary production, are found in response to a rapid increase of SST for the period 1998–2018 (Bates & Johnson, 2020; D'Alelio et al., 2020).

Because of the well-known photoacclimation processes's strong influence in the subtropical gyres (Barbieux et al., 2018), the use of $b_{bp}$ and of CHL:$b_{bp}$ ratio could help to understand the reported temporal patterns. Indeed, it is known that $b_{bp}$ is a better proxy to describe phytoplankton carbon biomass, $C_{phyto}$ (e.g., Behrenfeld et al., 2005; Bellacicco et al., 2020; Westberry et al., 2008) respect to CHL alone, hence can help to distinguish between phytoplankton standing stocks and physiological adjustment (see Figure 1 in Bellacicco et al., 2016). In Figure 4 (continuous lines), it can be observed how the $b_{bp}$ time series shows a different temporal pattern in respect to CHL, exhibiting its maximum values in initial years of ∼1.1·$10^{-3}$ $m^{-1}$, followed by a strong decrease, and then remaining fairly stable around 0.9·$10^{-3}$ $m^{-1}$ from 2003 onwards showing range of magnitude comparable with previous works (Bellacicco et al., 2018; Dall'Olmo et al., 2012). Here, the CHL:$b_{bp}$ ratio experiences an increase until 2004, followed by a slight descending but fairly stable phase until 2010, after which it decreases almost linearly until the end of the series (Figure 4; Figures S5–S7 in Supporting Information S1). The CHL: $b_{bp}$ increase until 2004 can't be unraveled as distinctly. As a matter of fact, since in those years the ultra-oligotrophic waters are very limited in space, this behavior may be related to different causes that cannot be disentangled, for example, a non-conserved particle size distribution, or a strong contribution of non-algal backscattering particles (Bellacicco et al., 2019) as well as a mix of variations of phytoplankton biomass and physiological adaptation. From 2010 to 2012, the CHL: $b_{bp}$ reduction could be mostly driven by phytoplankton standing stock changes. This could be due to the concurrent drop-off of SST to minimum values (which can be interpreted as a surrogate of nutrient stress; Switzer et al., 2003) together with CHL highest values and corresponding $b_{bp}$ increasing until 2012. The following CHL:$b_{bp}$ reduction, until 2014, could be interpreted mostly due to physiology adaptation of phytoplankton to the rapid increase of SST that reach its maximum values (and consequent high nutrient stress) which impact particularly the core of the area under study (Figures S5–S7 in Supporting Information S1) with concurrent slight deepening of MLD coupled to a sharp enhancement of $z_{SD}$ (and indirectly light availability). Light-harvesting components are rich in nitrogen, making CHL an expensive-nitrogen investment for a cell when nutrients are limited. In this period, nutrients are limited due to the SST increase, while light availability is not, so phytoplankton do not need more CHL to photosynthesize and CHL:$b_{bp}$ tends to decrease (Behrenfeld et al., 2005).

On the other hand, $z_{SD}$ shows a reversed regime if compared to $b_{bp}$ with an overall increase during the whole period, ranging from its minimum of 45 m in 1998 and reaching its maximum of 48 m in the latest years, accounting for a slight increment of transparency confirming what has been observed by Boyce et al. (2010, 2014) and recently in Pitarch et al. (2021). Similarly, MLD encountered a deepening in the whole 1998–2018 period, ranging from its lower values of 19–20 m in the early years to its higher values of 26–27 m at the end of the series, being positively correlated with SST (0.59; Figure S4 in Supporting Information S1) and indicating that the role played by warming waters as a driver of oligotrophic condition is not through a local stratification increase. Such increase is completely in accordance with low phytoplankton CHL concentration since the light availability and nutrient supply induced by vertical mixing for phytoplankton is necessarily limited (i.e., the nitracline is located around 100 m; Organelli & Claustre, 2019), and values are in the range reported by Palter et al. (2005), Dave and Lozier (2013), and Dave et al. (2015). It is to be noted that the slight deepening of the MLD of around 6–7 m, is possibly modulated by weather conditions such as the increased wind stress in the North Atlantic area (Lozier et al., 2011; Figure S4 in Supporting Information S1).

Even if in the entire region SST results to be fairly stable during the 21 years analyzed, when evaluating its average value in the restricted ultra-oligotrophic region the series does show a higher variability and a clear increase (Figure 4f and Figure S5 in Supporting Information S1). It is also of importance, if thinking of ocean warming

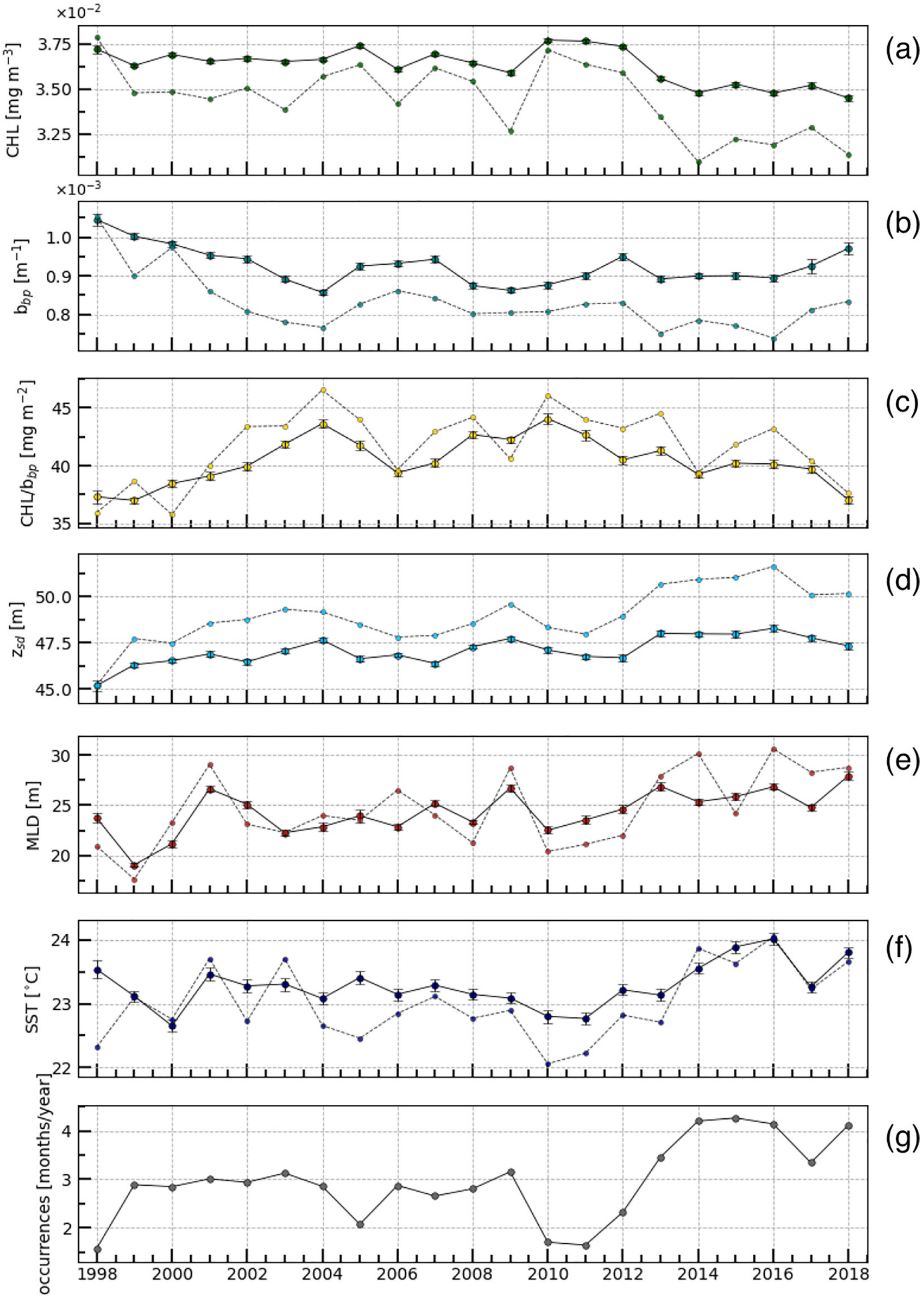


**Figure 4.** Time series of annual (a) chlorophyll-*a* (CHL), (b) $b_{bp}$, (c) CHL:$b_{bp}$ ratio, (d) $z_{SD}$, (e) Mixed Layer Depth, and (f) Sea Surface Temperature averaged where CHL ≤ 0.04 mg $m^{-3}$ during the 1998–2018 period, and for the red fixed area of Figure 3 (dashed lines). Average annual occurrences are shown in the last panel (g).

as the main forcing in the area of the environmental inter-annual long-term variability (Boyce et al., 2014), in particular of CHL variations, to consider the fact that the 21 years under analysis in our work, 1998–2018, are actually part of a longer warming oscillation. This can be evidenced by already looking at the complete ESA CCI SST data set, which covers nearly 40 years from 1982 to present. A linear trend of $0.02 \pm 0.002$°C/yr in the North Atlantic Ocean is shown in Figure S8 in Supporting Information S1. When analyzing a longer temporal SST series given by the HadISST 1850-onwards data set, this long-varying warming oscillation is even more evident, and clearly suggests this tendency condition in the North Atlantic will sharpen.

Consistent results are obtained for all time series also when evaluating variables over the largest fixed box which shows non-null occurrences of CHL $\leq 0.04$ mg m$^{-3}$ during all years (Figure 4, dashed lines). All time series depicted in Figure 4 include confidence intervals on the annual averages estimated through a bootstrapping procedure based on a Monte Carlo approach implying 1,000 resamples with replacement (Efron & Tibshirani, 1993), attaining at least two orders of magnitude lower than the annual average values.

## 4. Conclusions and Future Perspectives

The main conclusions of this work are:

- Previously published articles that investigated the areal increase of oligotrophic waters in the oceanic subtropical gyres used CHL thresholds of 0.07 or 0.1 mg m$^{-3}$ to define the oligotrophic regime. Since these limits do characterize the NASTG in all months, they do not allow observing the expansion of the oligotrophic condition in the area (Polovina et al., 2008), hence motivating our study to focus on the most oligotrophic waters characterized by CHL $\leq 0.04$ mg m$^{-3}$. Furthermore, since environmentally driven physiology plays an important role in the CHL patterns, rather than changes in biomass, we suggest the coupled use of CHL and $b_{bp}$ as important to understand phytoplankton dynamics and trophic status changes.
- In the last 21 years, low CHL waters (CHL $\leq 0.04$ mg m$^{-3}$) have displayed a non-linear change pattern, though overall expanding in space and increasing in frequency, with respect to the beginning of the time series, accounting for an area growth of around 96.3% and an increase of average monthly occurrences per year of 53.8% (Figures 2 and 3). This expansion and prevalence tendency is found to be concurrent with a marked increase of SST (Figure 4), but also associated with a deepening of the MLD. These observations thus point to a role of ocean warming in determining a sharpening of the oligotrophic conditions within the subtropical gyre that is more complex than the local stratification increase and vertical nutrient flux reduction.

Future work in this pathway may include: (a) combination of long-term satellite data and multi-years autonomous platforms observations (e.g., Biogeochemical-Argo floats) to better understand how ocean warming impacts the ocean biology of the NASTG along the fourth-dimension of the ocean, coupling biogeochemical and physical variables and (b) to quantify and characterize the impact of the ultra-oligotrophic waters expansion on the biological carbon pump (carbon exports) in the NASTG over the last decades.

## Data Availability Statement

Daily $R_{rs}$ and CHL Level 3 can be found at: https://catalogue.ceda.ac.uk/uuid/99348189bd33459cb-d597a58c30d8d10. Monthly Level 3 $z_{SD}$ data set can be found at: https://doi.org/10.1594/PANGAEA.904266. ESA CCI SST Level 4 can be found at: http://dx.doi.org/10.5285/62c0f97b1eac4e0197a674870afe1ee6. HadISST data set can be found at: https://doi.org/10.5065/XMYE-AN84. ARMOR3d MLD is available at https://doi.org/10.48670/moi-00052. Monthly CHL, $b_{bp}$, $z_{SD}$, and MLD data at 25 km resolution optimally interpolated for the North Atlantic Ocean can be found at the following link: https://doi.org/10.5281/zenodo.6326109. Codes to replicate Figures 2–4 are freely available at https://doi.org/10.5281/zenodo.6327488.

**Acknowledgments**

This work was funded by the ESA Living Planet Fellowship Project PHYSI-OGLOB: *Assessing the inter-annual physiological response of phytoplankton to global warming using long-term satellite observations*, 2018–2020 and supported by H2020 project AtlantECO (Grant 862923). We would like to thank ESA CCI (https://climate.esa.int/en/odp/#/dashboard), CMEMS (https://resources.marine.copernicus.eu/products), and UK MetOffice (https://www.metoffice.gov.uk/hadobs/hadisst/) for providing state-of-art data. We also thank Dr. Gael Forget and the anonymous reviewer for their suggestions and inputs that helped the manuscript to be improved.

## References

Barbieux, M., Uitz, J., Bricaud, A., Organelli, E., Poteau, A., Schmechtig, C., et al. (2018). Assessing the variability in the relationship between the particulate backscattering coefficient and the chlorophyll a concentration from a global biogeochemical-Argo database. *Journal of Geophysical Research: Oceans*, *123*(2), 1229–1250. https://doi.org/10.1002/2017jc013030

Bates, N. R., & Johnson, R. J. (2020). Acceleration of ocean warming, salinification, deoxygenation and acidification in the surface subtropical North Atlantic Ocean. *Communications Earth & Environment*, *1*(1), 1–12. https://doi.org/10.1038/s43247-020-00030-5

Behrenfeld, M. J., Boss, E., Siegel, D. A., & Shea, D. M. (2005). Carbon-based ocean productivity and phytoplankton physiology from space. *Global Biogeochemical Cycles*, *19*(1), GB1006. https://doi.org/10.1029/2004gb002299

Behrenfeld, M. J., O'Malley, R. T., Boss, E. S., Westberry, T. K., Graff, J. R., Halsey, K. H., et al. (2015). Revaluating ocean warming impacts on global phytoplankton. *Nature Climate Change*, *6*(3), 323–330. https://doi.org/10.1038/nclimate2838

Behrenfeld, M. J., O'Malley, R. T., Siegel, D. A., McClain, C. R., Sarmiento, J. L., Feldman, G. C., et al. (2006). Climate-driven trends in contemporary ocean productivity. *Nature*, *444*(7120), 752–755. https://doi.org/10.1038/nature05317

Bellacicco, M., Cornec, M., Organelli, E., Brewin, R. J. W., Neukermans, G., Volpe, G., et al. (2019). Global variability of optical backscattering by non-algal particles from a biogeochemical-Argo data set. *Geophysical Research Letters*, *46*(16), 9767–9776. https://doi.org/10.1029/2019gl084078

Bellacicco, M., Pitarch, J., Organelli, E., Martinez-Vicente, V., Volpe, G., & Marullo, S. (2020). Improving the retrieval of carbon-based phytoplankton biomass from satellite ocean colour observations. *Remote Sensing*, *12*(21), 3640. https://doi.org/10.3390/rs12213640

Bellacicco, M., Volpe, G., Briggs, N., Brando, V., Pitarch, J., Landolfi, A., et al. (2018). Global distribution of non-algal particles from ocean color data and implications for phytoplankton biomass detection. *Geophysical Research Letters*, *45*(15), 7672–7682. https://doi.org/10.1029/2018gl078185

Bellacicco, M., Volpe, G., Colella, S., Pitarch, J., & Santoleri, R. (2016). Influence of photoacclimation on the phytoplankton seasonal cycle in the Mediterranean Sea as seen by satellite. *Remote Sensing of Environment*, *184*, 595–604. https://doi.org/10.1016/j.rse.2016.08.004

Boyce, D. G., Dowd, M., Lewis, M. R., & Worm, B. (2014). Estimating global chlorophyll changes over the past century. *Progress in Oceanography*, *122*, 163–173. https://doi.org/10.1016/j.pocean.2014.01.004

Boyce, D. G., Lewis, M. R., & Worm, B. (2010). Global phytoplankton decline over the past century. *Nature*, *466*(7306), 591–596. https://doi.org/10.1038/nature09268

D'Alelio, D., Rampone, S., Cusano, L. M., Morfino, V., Russo, L., Sanseverino, N., et al. (2020). Machine learning identifies a strong association between warming and reduced primary productivity in an oligotrophic ocean gyre. *Scientific Reports*, *10*(1), 1–12. https://doi.org/10.1038/s41598-020-59989-y

Dall'Olmo, G., Boss, E., Behrenfeld, M. J., & Westberry, T. K. (2012). Particulate optical scattering coefficients along an Atlantic meridional transect. *Optics Express*, *20*(19), 21532–21551. https://doi.org/10.1364/oe.20.021532

Dave, A. C., Barton, A. D., Lozier, M. S., & McKinley, G. A. (2015). What drives seasonal change in the oligotrophic area in the subtropical North Atlantic? *Journal of Geophysical Research: Oceans*, *120*(6), 3958–3969. https://doi.org/10.1002/2015jc010787

Dave, A. C., & Lozier, M. S. (2013). Examining the global record of interannual variability in stratification and marine productivity in the low-latitude and mid-latitude ocean. *Journal of Geophysical Research: Oceans*, *118*(6), 3114–3127. https://doi.org/10.1002/jgrc.20224

Donlon, C. J., Martin, M., Stark, J., Roberts-Jones, J., Fiedler, E., & Wimmer, W. (2012). The operational sea surface temperature and sea ice analysis (OSTIA) system. *Remote Sensing of Environment*, *116*, 140–158. https://doi.org/10.1016/j.rse.2010.10.017

Dutkiewicz, S., Hickman, A. E., Jahn, O., Henson, S., Beaulieu, C., & Monier, E. (2019). Ocean colour signature of climate change. *Nature Communications*, *10*(1), 1–13. https://doi.org/10.1038/s41467-019-08457-x

Efron, B., & Tibshirani, R. J. (1993). *An introduction to the bootstrap* (p. 456). Chapman & Hall, CRC Press.

Ghil, M., Allen, M. R., Dettinger, M. D., Ide, K., Kondrashov, D., Mann, M. E., et al. (2002). Advanced spectral methods for climatic time series. *Reviews of Geophysics*, *40*(1), 1003–3-41. https://doi.org/10.1029/2000RG000092

Gregg, W. W., Casey, N. W., & McClain, C. R. (2005). Recent trends in global ocean chlorophyll. *Geophysical Research Letters*, *32*(3), L03606. https://doi.org/10.1029/2004gl021808

Gregg, W. W., & Conkright, M. E. (2002). Decadal changes in global ocean chlorophyll. *Geophysical Research Letters*, *29*(15), 20–21. https://doi.org/10.1029/2002gl014689

Guinehut, S., Dhomps, a.-L., Larnicol, G., & Le Traon, P.-Y. (2012). High resolution 3-D temperature and salinity fields derived from in situ and satellite observations. *Ocean Science*, *8*(5), 845–857. https://doi.org/10.5194/os-8-845-2012

Halsey, K. H., & Jones, B. M. (2015). Phytoplankton strategies for photosynthetic energy allocation. *Annual Review of Marine Science*, *7*(1), 265–297. https://doi.org/10.1146/annurev-marine-010814-015813

Henson, S. A., Sanders, R., & Madsen, E. (2012). Global patterns in efficiency of particulate organic carbon export and transfer to the deep ocean. *Global Biogeochemical Cycles*, *26*(1), GB1028. https://doi.org/10.1029/2011gb004099

Irwin, A. J., & Oliver, M. J. (2009). Are ocean deserts getting larger? *Geophysical Research Letters*, *36*(18), L18609. https://doi.org/10.1029/2009gl039883

Kondrashov, D., & Ghil, M. (2006). Spatio-temporal filling of missing points in geophysical data sets. *Nonlinear Processes in Geophysics*, *13*(2), 151–159. https://doi.org/10.5194/npg-13-151-2006

Kondrashov, D., Shprits, Y., & Ghil, M. (2010). Gap filling of solar wind data by singular spectrum analysis. *Geophysical Research Letters*, *37*(15). https://doi.org/10.1029/2010gl044138

Lee, Z., Shang, S., Hu, C., Du, K., Weidemann, A., Hou, W., et al. (2015). Secchi disk depth: A new theory and mechanistic model for underwater visibility. *Remote Sensing of Environment*, *169*, 139–149. https://doi.org/10.1016/j.rse.2015.08.002

Lozier, M. S., Dave, A. C., Palter, J. B., Gerber, L. M., & Barber, R. T. (2011). On the relationship between stratification and primary productivity in the North Atlantic. *Geophysical Research Letters*, *38*(18), L18609. https://doi.org/10.1029/2011gl049414

Martinez, E., Antoine, D., D'Ortenzio, F., & Gentili, B. (2009). Climate-driven basin-scale decadal oscillations of oceanic phytoplankton. *Science*, *326*(5957), 1253–1256. https://doi.org/10.1126/science.1177012

McClain, C. R., Signorini, S. R., & Christian, J. R. (2004). Subtropical gyre variability observed by ocean-color satellites. *Deep Sea Research Part II: Topical Studies in Oceanography*, *51*(1–3), 281–301. https://doi.org/10.1016/j.dsr2.2003.08.002

Merchant, C. J., Embury, O., Bulgin, C. E., Block, T., Corlett, G. K., Fiedler, E., et al. (2019). Satellite-based time-series of sea-surface temperature since 1981 for climate applications. *Scientific Data*, *6*(1), 1–18. https://doi.org/10.1038/s41597-019-0236-x

Merchant, C. J., Embury, O., Roberts-Jones, J., Fiedler, E., Bulgin, C. E., Corlett, G. K., et al. (2014). Sea surface temperature datasets for climate applications from phase 1 of the European Space Agency Climate Change Initiative (SST CCI). *Geoscience Data Journal*, *1*(2), 179–191. https://doi.org/10.1002/gdj3.20

Organelli, E., & Claustre, H. (2019). Small phytoplankton shapes colored dissolved organic matter dynamics in the North Atlantic subtropical gyre. *Geophysical Research Letters*, *46*(21), 12183–12191. https://doi.org/10.1029/2019GL084699

Organelli, E., Dall'Olmo, G., Brewin, R. J., Nencioli, F., & Tarran, G. A. (2020). Drivers of spectral optical scattering by particles in the upper 500 m of the Atlantic Ocean. *Optics Express*, *28*(23), 34147–34166. https://doi.org/10.1364/oe.408439

Organelli, E., Dall'Olmo, G., Brewin, R. J., Tarran, G. A., Boss, E., & Bricaud, A. (2018). The open-ocean missing backscattering is in the structural complexity of particles. *Nature Communications*, *9*(1), 1–11. https://doi.org/10.1038/s41467-018-07814-6

Palter, J. B., Lozier, M. S., & Barber, R. T. (2005). The effect of advection on the nutrient reservoir in the North Atlantic subtropical gyre. *Nature*, *437*(7059), 687–692. https://doi.org/10.1038/nature03969

Pitarch, J., Bellacicco, M., Marullo, S., & van der Woerd, H. J. (2021). Global maps of Forel–Ule index, hue angle and Secchi disk depth derived from 21 years of monthly ESA Ocean Colour Climate Change Initiative data. *Earth System Science Data*, *13*(2), 481–490. https://doi.org/10.5194/essd-13-481-2021

Pitarch, J., Bellacicco, M., Organelli, E., Volpe, G., Colella, S., Vellucci, V., & Marullo, S. (2020). Retrieval of particulate backscattering using field and satellite radiometry: Assessment of the QAA algorithm. *Remote Sensing*, *12*(1), 77. https://doi.org/10.3390/rs12010077

Pitarch, J., van der Woerd, H. J., Brewin, R. J. W., & Zielinski, O. (2019). Twenty years of monthly global maps of Hue angle, Forel-Ule and Secchi disk depth, based on ESA-OC-CCI data [Dataset]. PANGAEA. https://doi.org/10.1594/PANGAEA.904266

Polovina, J. J., Howell, E. A., & Abecassis, M. (2008). Ocean's least productive waters are expanding. *Geophysical Research Letters*, *35*(3), L03618. https://doi.org/10.1029/2007gl031745

Sathyendranath, S., Brewin, R. J., Brockmann, C., Brotas, V., Calton, B., Chuprin, A., et al. (2019). An ocean-colour time series for use in climate studies: The experience of the Ocean-Colour Climate Change Initiative (OC-CCI). *Sensors*, *19*(19), 4285. https://doi.org/10.3390/s19194285

Siegel, D. A., Behrenfeld, M. J., Maritorena, S., McClain, C. R., Antoine, D., Bailey, S. W., et al. (2013). Regional to global assessments of phytoplankton dynamics from the SeaWiFS mission. *Remote Sensing of Environment*, *135*, 77–91. https://doi.org/10.1016/j.rse.2013.03.025

Stramski, D., Boss, E., Bogucki, D., & Voss, K. J. (2004). The role of seawater constituents in light backscattering in the ocean. *Progress in Oceanography*, *61*(1), 27–56. https://doi.org/10.1016/j.pocean.2004.07.001

Switzer, A. C., Kamykowski, D., & Zentara, S. J. (2003). Mapping nitrate in the global ocean using remotely sensed sea surface temperature. *Journal of Geophysical Research*, *108*(C8), 3280. https://doi.org/10.1029/2000jc000444

Westberry, T., Behrenfeld, M. J., Siegel, D. A., & Boss, E. (2008). Carbon-based primary productivity modeling with vertically resolved photoacclimation. *Global Biogeochemical Cycles*, *22*(2), GB2024. https://doi.org/10.1029/2007GB003078

WMO. (2017). WMO guidelines on the calculation of climate normals.

## References From the Supporting Information

Beckers, J. M., & Rixen, M. (2003). EOF calculations and data filling from incomplete oceanographic datasets. *Journal of Atmospheric and Oceanic Technology*, *20*(12), 1839–1856. https://doi.org/10.1175/1520-0426(2003)020<1839:ecadff>2.0.co;2

de Boyer Montégut, C., Madec, G., Fischer, A. S., Lazar, A., & Iudicone, D. (2004). Mixed layer depth over the global ocean: An examination of profile data and a profile-based climatology. *Journal of Geophysical Research*, *109*(C12), C12003. https://doi.org/10.1029/2004JC002378

de Boyer Montégut, C., Mignot, J., Lazar, A., & Cravatte, S. (2007). Control of salinity on the mixed layer depth in the world ocean: 1. General description. *Journal of Geophysical Research*, *112*(C6), C06011. https://doi.org/10.1029/2006JC003953

Droghei, R., Buongiorno Nardelli, B., & Santoleri, R. (2018). A new global sea surface salinity and density dataset from multivariate observations (1993–2016). *Frontiers in Marine Science*, *5*(March), 1–13. https://doi.org/10.3389/fmars.2018.00084

Groth, A., Feliks, Y., Kondrashov, D., & Ghil, M. (2017). Interannual variability in the North Atlantic Ocean's temperature field and its association with the wind stress forcing. *Journal of Climate*, *30*(7), 2655–2678. https://doi.org/10.1175/jcli-d-16-0370.1

Mignot, J., de Boyer Montégut, C., Lazar, A., & Cravatte, S. (2007). Control of salinity on the mixed layer depth in the world ocean: 2. Tropical areas. *Journal of Geophysical Research*, *112*(C10), C10010. https://doi.org/10.1029/2006JC003954

Rayner, N. A. A., Parker, D. E., Horton, E. B., Folland, C. K., Alexander, L. V., Rowell, D. P., et al. (2003). Global analyses of sea surface temperature, sea ice, and night marine air temperature since the late nineteenth century. *Journal of Geophysical Research*, *108*(D14), 4407. https://doi.org/10.1029/2002jd002670

Taburet, G., Sanchez-Roman, A., Ballarotta, M., Pujol, M. I., Legeais, J. F., Fournier, F., et al. (2019). DUACS DT2018: 25 years of reprocessed sea level altimetry products. *Ocean Science*, *15*(5), 1207–1224. https://doi.org/10.5194/os-15-1207-2019